

## MISR DECADAL OBSERVATIONS OF MINERAL DUST: PROPERTY CHARACTERIZATION AND CLIMATE APPLICATIONS

Olga V. Kalashnikova<sup>A</sup>, Michael J. Garay<sup>B</sup>, Irina Sokolik<sup>C</sup>, Ralph A. Kahn<sup>D</sup>, A. Lyapustin<sup>D</sup>, David J. Diner<sup>B</sup>, Jae N. Lee<sup>D</sup>, Omar Torres<sup>D</sup>, Gregory G. Leptoukh<sup>D</sup>, and Ismail Sabbah<sup>E</sup>

<sup>A</sup>Corresponding author Email: Olga.V.Kalashnikova@jpl.nasa.gov

<sup>A</sup>Jet Propulsion Laboratory, California Institute of Technology, Pasadena, California, USA

<sup>B</sup>Jet Propulsion Laboratory, California Institute of Technology, Pasadena, California, USA

<sup>C</sup>School of Earth and Atmospheric Sciences, Georgia Institute of Technology, Atlanta, Georgia, USA

<sup>D</sup>NASA Goddard Space Flight Center, Greenbelt, Maryland, USA

<sup>E</sup>Department of Natural Sciences, College of Health Sciences, the Public Authority of Applied Education and Training, Kuwait

### Abstract

The Multi-angle Imaging SpectroRadiometer (MISR) provides a unique, independent source of data for studying dust emission and transport. MISR's multiple view angles allow the retrieval of aerosol properties over bright surfaces, and such retrievals have been shown to be sensitive to the non-sphericity of dust aerosols over both land and water. MISR stereographic views of thick aerosol plumes allow height and instantaneous wind derivations at spatial resolutions of better than 1.1 km horizontally and ~200m vertically. We will discuss the radiometric and stereo-retrieval capabilities of MISR specifically for dust, and demonstrate the use of MISR data in conjunction with other available satellite observations for dust property characterization and climate studies.

First, we will discuss MISR non-spherical (dust) fraction product over the global oceans. We will show that over the Atlantic Ocean, changes in the MISR-derived non-spherical AOD fraction illustrate the evolution of dust during transport. Next, we will present a MISR satellite perspective on dust climatology in major dust source regions with a particular emphasis on the West Africa and Middle East and discuss MISR's unique strengths as well as current product biases. Finally, we will discuss MISR dust plume product and climatological applications.

Keywords: MISR, non-spherical fraction, MINX, dust sources, dust plumes

© 2012. All rights reserved.

## **1. INTRODUCTION**

Despite its well-recognized importance, the impact of mineral aerosol (dust) on the environment and its relation to global climate factors and synoptic scale systems remains difficult to quantify. The 12+ years of observations from the Multi-angle Imaging SpectroRadiometer (MISR) instrument on the polar-orbiting Terra satellite provide a unique, independent source of data for studying dust emissions and transport. MISR's multiple view angles allow the simultaneous retrieval of dust plume top height and dust motion during the seven minutes a scene is in view. In addition, MISR retrieves aerosol properties over bright surfaces, and such retrievals have been shown to be sensitive to the non-sphericity of dust aerosols.

We examine the MISR 12+ year aerosol data record to demonstrate MISR's unique strengths and assess potential biases of MISR products for dust study applications, with a particular focus on the Sahara and the Middle East. In particular, we examine MISR's unique capabilities to: 1) distinguish dust aerosol from spherical aerosol types, 2) provide aerosol optical depth (AOD) over bright desert source regions, and 3) provide high-resolution retrievals of dust plume heights and associated winds. We show examples of regional and global MISR data products in dusty regions together with quantitative evaluations of product accuracies through comparisons with independent data sources, and discuss applications of MISR data to dust regional and climatological studies, such as dust property evolution during transport, dust source climatology, and dust source dynamics.

## **2. MISR SPECIFICATIONS AND PRODUCTS**

MISR is a multi-angle imaging instrument consisting of nine cameras with view angles of 70.5, 60.0, 45.6, 26.1, and 0 (nadir), operating in four spectral bands centered at 446 nm (blue), 558 nm (green), 672 nm (red), and 867 nm (near infrared). In global observing mode, the spatial resolution of the red band is 275 m in all nine cameras, the other bands are re-sampled to 1.1 km resolution in all the cameras, except the nadir, which preserves the full 275 m resolution in all four bands. The common swath width is ~400 km and global coverage is obtained every nine days at the equator and more frequently at higher latitudes (Diner et al., 1998). MISR benefits from its multi-angle capabilities to perform simultaneous retrievals of aerosol and surface properties over bright surfaces. A number of validation studies have shown that MISR AOD is reliable (accuracy on the order of  $\pm 0.05$ ) over desert sites (Martonchik et al., 2004; Xia et al., 2008). MISR aerosol plume top height and wind information (including dust plumes) are derived at a spatial resolution of 1.1 x 1.1 km by analysis of the MISR radiance data using the MISR Interactive eXplorer (MINX) tool (Nelson et al., 2008a; 2008b).

## **3. MISR NON-SPHERICAL FRACTION PRODUCT**

Multiangle, multispectral radiances observed by MISR enable distinguishing between spherical anthropogenic and non-spherical dust particles (Kahn et al., 1998; Kahn et al., 2001; Kalashnikova et al., 2005). The MISR aerosol retrieval algorithm can distinguish non-spherical dust from other spherical aerosol components as the instrument measures the angular distribution of the backscattered, top of atmosphere, radiances modified by the presence of non-spherical particles (Kalashnikova et al., 2005; Kalashnikova and Kahn, 2006). Previous theoretical and case studies have demonstrated that under good viewing conditions over dark water the MISR aerosol retrieval is sensitive to differences in the angular-spectral signals of medium-mode dust shapes when the mid-visible AOD is larger than about 0.15, for components contributing 15-20% or more to the total AOD (Kalashnikova and Kahn, 2006). The highest quality MISR AOD non-spherical fraction retrievals (i.e., the non-spherical fraction multiplied by the total AOD) are

found when the mid-visible AOD is larger than about 0.5 – conditions when atmospheric aerosols dominate the TOA radiances. However, the observed scattering angles, the scattering angle range, and the number of cameras available for aerosol retrievals can all significantly affect the MISR AOD non-spherical fraction retrieval because the angular-based particle distinguishability is a strong function of a viewing geometry, especially over the ocean.

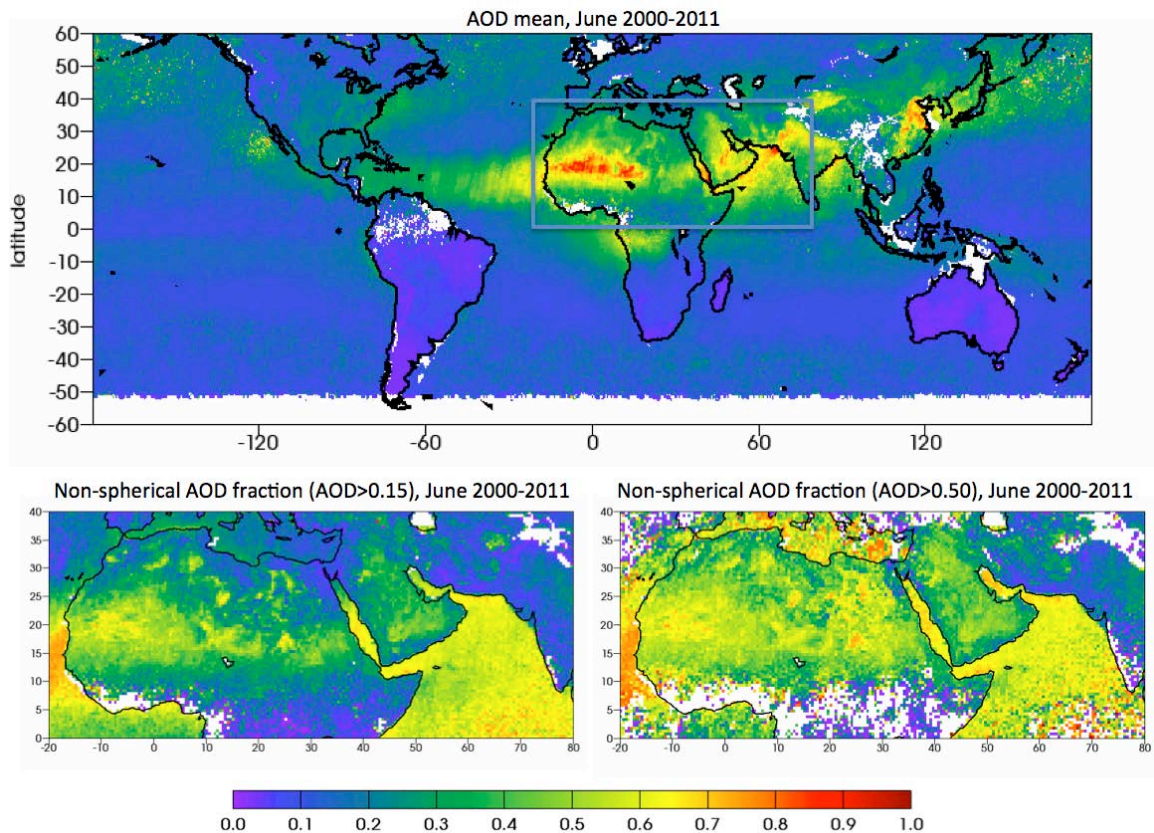


*Figure 1. MISR AOD (top), non-spherical AOD fraction for AOD>0.15 (lower left), and non-spherical AOD fraction for AOD>0.5 (lower right) gridded on a 0.5° grid and averaged over 12 years of observations (2000-2011).*

The number of representative MISR and ground-based AERONET sunphotometer property retrievals coincident in time and space is limited, and is not statistically representative enough to perform a global validation of the non-spherical fraction. Therefore, we qualitatively examine the global MISR non-sphericity patterns obtained from 11+ years of observations to evaluate spatiotemporal distributions against known, climatological distributions of dust aerosol. As an example of our assessment, Figure 1 shows the global distribution of MISR AOD for June gridded on a 0.5° grid and averaged over 12 years of observations (2000-2011). This is plotted together with non-spherical AOD fraction over the Sahara and Middle East.

Figure 1 demonstrates that the MISR aerosol non-sphericity product identifies Saharan and Middle East dust in regions where dust is expected. However, some land-water discontinuity in the dust fraction is apparent. We can explain the observed discontinuity from results obtained from theoretical sensitivity studies. The MISR aerosol retrieval algorithm is sensitive to differences in the spectral signals of medium-mode dust with different composition (amount of hematite) at short visible wavelengths (blue and green), but there is very little difference in the spectral signature of dust of different compositions at wavelengths longer than 0.6  $\mu\text{m}$ . The

current MISR aerosol retrieval algorithm uses two channels (red and near infrared) for water retrievals and all 4 channels (blue, green, red, and near infrared) for land retrievals; therefore the retrieval sensitivity to dust composition is expected to change across land-water boundaries. The dust model with a fixed refractive index that is currently used in the operational MISR aerosol look up table (LUT) is a valid assumption for 2-wavelength water retrievals; however, a wider range of dust models reflecting regional variability of dust chemistry (e.g., refractive index) likely needs to be included in the LUT to optimize the performance of 4-band land retrievals in different parts of the globe. The MISR "blue" wavelength dust optical properties are also not consistent with the optical properties calculated for the other three band, potentially limiting the performance of the dust optical model over some types of land surface.

The theoretical studies also demonstrated that MISR non-spherical fraction is more reliable over water than land, and more reliable over the Sahara and Middle East compared with mid-latitude Asia. This could be partially due to MISR sensitivities at different viewing geometries, and partially by the inability of a single dust optical model to represent regional differences in dust optical properties.

MISR-derived aerosol non-sphericity is useful for studying the behavior of transported dust. However, note that relative changes in non-sphericity during dust transport are more reliable than the absolute dust non-spherical AOD values. We have demonstrated that MISR-constrained dust properties remain unchanged during five days of trans-Atlantic transport for the selected cases of dust sampled progressively downwind (Kalashnikova and Kahn, 2008).

#### **4. MISR AOD DATA QUALITY OVER BRIGHT SURFACES**

The performance of the operational MISR aerosol retrieval over bright desert sources and its sensitivity to near surface aerosols and surface properties have been validated and used over many desert surfaces (e.g., Martonchik et al., 2004; Frank et al., 2007; Christopher et al., 2008; Kahn et al., 2009). A global comparison of coincident MISR and AERONET sunphotometer data showed that overall, about 70% to 75% of MISR AOD retrievals fall within the larger of 0.05 or 20% of AOD, and about 50% to 55% are within the larger of 0.03 or 10% AOD, except at sites where dust or mixed dust and smoke are commonly found (Kahn et al., 2010). Figure 2 shows the AOD difference plot for all available 2000-2010 MISR mid-visible (green band) AOD against coincident AERONET AOD measurements (interpolated to MISR green band) in the 3 by 3 nearest 17.6 km MISR aerosol retrieval regions and within  $\pm 1$  hour of the MISR overpass for West African and Middle East AERONET stations. There are 1698 collocation data points at AERONET stations in the West Africa and 1713 collocation data points at AERONET stations in the Middle East.

Consistent with previous, global studies, MISR retrievals in both dust-dominated regions tend to overestimate instantaneous AOD in the low AOD range (below 0.1) and underestimate it in the high AOD range (greater than 0.7) compared to the AERONET AOD (Kahn et al., 2010). A greater diversity of dust optical models is needed for the MISR algorithm to better represent different desert source regions, though other factors might also be involved. For the dusty AERONET sites 54.06 % (West Africa) and 49.74 % (Middle East) are within the larger of 0.05 or 20% of the AOD, and 77.44 % (West Africa) and 80.85% (Middle East) are within the larger of 0.1 or 30% of the AOD.

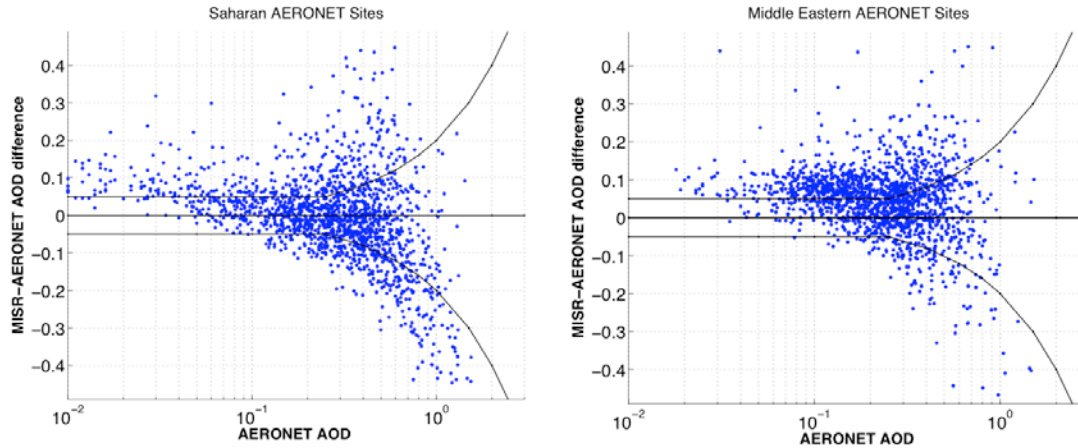


Figure 2. Difference plot showing comparisons between MISR land algorithm mid-visible (green-band) AOD retrieval results and near-coincident AERONET retrievals over Saharan AERONET sites and over Middle Eastern AERONET sites. Horizontal lines mark the zero difference and bracket the 0.05 or  $20\% \times \text{AOD}$  envelope.

Because the majority of MISR data falls in the AOD range above 0.1 and below 0.7 where the retrieval performs well (84.61% for the Middle East AERONET stations and 66.77% for the West Africa AERONET stations), MISR inter-annual and seasonal AOD patterns reproduce those at AERONET stations, and agree with independent satellite data in dust source regions (Carboni et al., 2012). Recent studies have shown that the operational MISR aerosol product provides reliable climatology in Africa and the Middle East that are of the sufficient quality to be used for model evaluation of dust AOD temporal and spatial variability (Marey et al., 2011; Yigiletu et al., 2011).

## 5. DUST PLUME DYNAMICS

MISR aerosol plume top height and wind information are derived at a spatial resolution of  $1 \times 1$  km by analysis of the MISR radiance data using the MISR Interactive eXplorer (MINX) tool (Nelson et al., 2008a, Nelson et al., 2008b). MINX provides an interface within which a trained user can outline dust plumes and provide a wind direction. Inclusion of the wind direction reduces the number of free parameters in the simultaneous stereoscopic retrieval of heights and winds from MISR data, allowing precise retrievals of the plume height and wind speed. Uncertainties in the plume heights are estimated to be  $\sim 200$  m, and uncertainties in the wind speed are  $\sim 1$ -2 m/s (Nelson et al., 2008b). As these high-resolution, spatially extensive measurements of dust plume-top heights are obtained geometrically, they are unaffected by background aerosols and thin cirrus, atmospheric thermal structure (e.g. temperature inversions), cloud emissivity, or instrument radiometric calibration. The MINX technique works well on the thick near-source plumes as well as on transported dust plumes that have sufficient spatial heterogeneity relative to the background so that they can be recognized by the pattern matching algorithm used by MINX.

Figure 3 shows two examples of comparisons of MINX dust plume heights with associated lidar data. The upper panel shows coincident in space and nearly coincident (3 hours difference) CALIPSO retrievals of aerosol type for 16 March 2009, a dust event over Pacific. The lower panel shows spatially and temporally coincident National Institute for Environmental Studies (NIES) ground-based lidar depolarization ratio observation over Japan on 2 April 2007. In both cases MISR-derived dust plume height and lidar observations place transported dust at 2.3-2.5km altitude. Note that the agreement is within the estimated 200 m uncertainty in the MINX retrieval

(the CALIPSO vertical resolution is 30 m). This figure shows that the MINX measurement uncertainty is applicable for dust plumes as well as for smoke plumes, which have been investigated previously (Nelson et. Al., 2008b). The MISR dust plume height and wind statistics may provide valuable constraints for testing and refining regional dust modeling systems and dust emission and lifting parameterizations within GCMs.

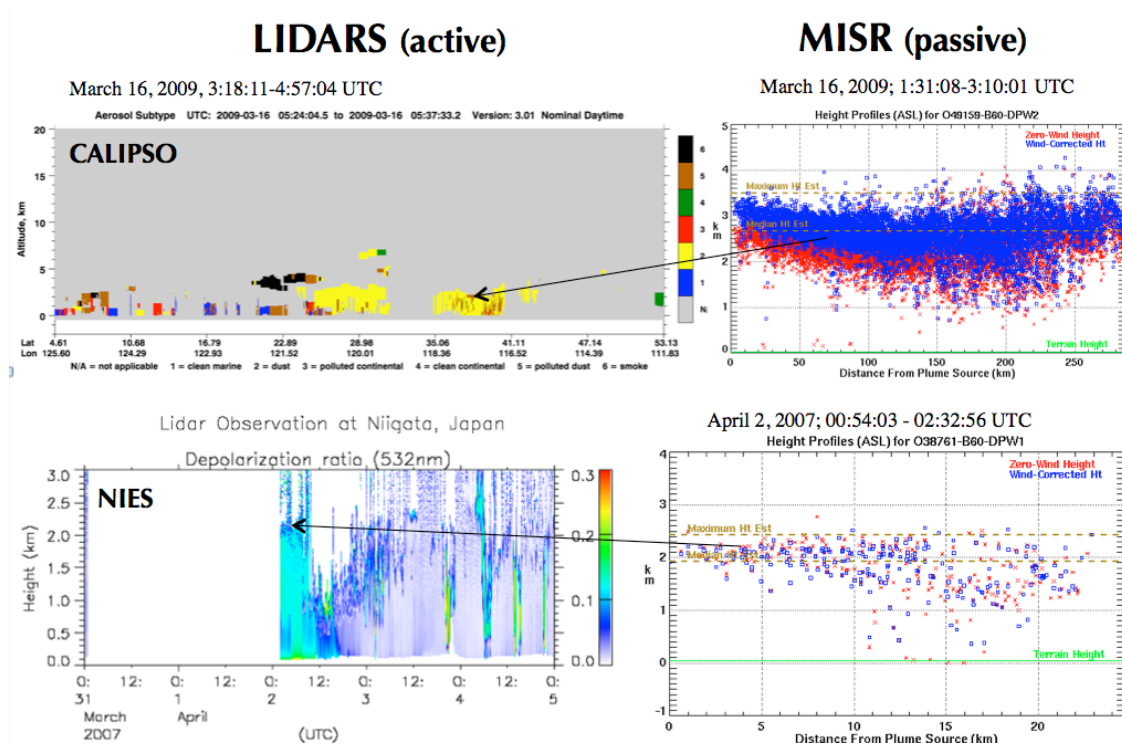


Figure 3. The comparison MISR MINX dust plume heights for the transported dust with a coincident in space and nearly coincident (3 hours difference) CALIPSO measurements of aerosol type (upper panel) and with coincident and space and time NIES ground-based lidar depolarization ratio (lower panel).

## 6. CONCLUSIONS

Analysis of the current (Version 22) MISR aerosol products shows that: 1) the MISR nonspherical fraction product performs well over water in terms of relative changes of dust fraction during transport over the Atlantic ocean, 2) MISR AOD retrievals fall within 0.1 or 30% of AOD in the low AOD range (AOD less than 0.5) in the arid dust-laden regions of North Africa and the Middle East, 3) MISR-derived dust plume heights and winds provide valuable insights on dust source dynamics.

## 6. ACKNOWLEDGEMENTS

We thank the MISR team for offering facilities, access to data, and useful discussions. The work of O. V. Kalashnikova is supported by in part by the NASA Earth Sciences Division, Climate and Radiation program, and in part by the NASA Earth Observing System Multiangle

Imaging SpectroRadiometer project, D. J. Diner, Principal Investigator. This work was performed at the Jet Propulsion Laboratory, California Institute of Technology, under contract with the National Aeronautics and Space Administration. The MISR data were obtained from the NASA Langley Research Center Atmospheric Sciences Data Center. I. Sabbah acknowledges (KFAS) Foundation for the Advancement of Sciences for their partial support of this research project (2011-1401-01).

## References

**Carboni, E., Thomas, G. E., Sayer, A. M., Siddans, R., Poulsen, C. A., Grainger, R. G., Ahn, C., Antoine, D., Bevan, S., Braak, R., Brindley, H., DeSouza-Machado, S., Deuzé, J. L., Diner, D., Ducos, F., Grey, W., Hsu, C., Kalashnikova, O. V., Kahn, R., North, P. R. J., Salustro, C., Smith, A., Tanré, D., Torres, O., and Veihelmann, B., 2012, Atmos. Meas. Tech., 5, 1973-2002, doi:10.5194/amt-5-1973-2012, 2012**

**Christopher, S. A., Gupta, P., and Haywood, J., 2008, J. Geophys. Res. 113 (D00C04), doi: 10.1029/2007JD009446.**

**Diner, D. J., et al., 1998, IEEE Trans. Geosci. Remote Sens., 36, 4, 1072–1087.**

**Diner, D. J., et al., 2004, Remote Sensing of Environment, 94, 155-171.**

**Frank, T. D., Girolamo, L. D., and Geegan, S., 2007, Rem. Sens. Environ 107, 54.**

**Kahn, R. A., West, R., McDonald, D., Rheingans, B., and Mishchenko, M., 1998, J. Geophys. Res. 102 , 16,86116,870**

**Kahn, R., Banerjee, P., and McDonald, D., 2001, J. Geophys. Res. 106 , 18,21918,238**

**Kahn, R. A., Gaitley, B. J., Garay, M. J., Diner, D. J., Eck, T. F., Smirnov, A., and Holben, B. N., 2010, J. Geophys. Res., 115, D23209, doi: 10.1029/2010JD014601.**

**Kahn, R., Petzold, A., Wendisch, M., Bierwirth, E., Dinter, T., Esselborn, M., Fiebig, M., Heese, B., Knippertz, P., Muller, D., Schladitz, A., and von Hoyningen-Huene, W., 2009, Tellus, 61, 239-251.**

**Kalashnikova, O. V., Kahn, R. A., Sokolik, I. N., and Li, W.-H., 2005, J. Geophys. Res. Vol. 110 , doi:10.1029/2004JD004550.**

**Kalashnikova, O. V. and Kahn, R. A., 2006, J. Geophys. Res. 111 (D11207), doi:10.1029/2005JD006756**

**Kalashnikova, O. V. and Kahn, R. A., 2008, J. Geophys. Res. 113. (D24204), doi:10.1029/2008JD010083**

**Martonchik, J. V., Diner, D. J., Kahn, R., Gaitley, B., and Holben, B., 2004,**

Geophys. Res. Lett. 31, doi:10.1029/2004GL019807.

**Marey, H. S., J. C. Gille, H. M. E.-A., Shalaby, E. A., and El-Raey, M. E., 2011,** Atmos. Chem. Phys. 11, 10637-10648, doi:10.5194/acp-11-10637-2011

**Nelson, D., Averill, C., Boland, S., Morford, R., Garay, M., Rheingans, B., Thompson, C., Hall, J., Diner, D., and Campbell, H., 2008,** JPL reports D-41552 (available from: <http://www.openchannelsoftware.com/projects/MINX>).

**Nelson, D. L., Chen, Y., Kahn, R. A., Diner, D. J., and Mazzoni, D., 2008,** Proc. of SPIE, 7089, doi: 10.1117/12.795087.

**Xia, X. G., Wang, P. C., and Wang, Y. S., 2008,** Geoph. Res. Lett. 35 (16), L16804.

**Yigiletu, M. T., Sivakumar, V., Botai, J. O., and Mengistu, G., 2011,** J. Geophys. Res., doi:10.1029/2011JD016023.